II. 研究成果の刊行に関する一覧表

研究成果の刊行に関する一覧表

書籍

著者氏名	論文タイトル名	書籍全体の編集者名	書　籍　名	出版社名	出版地	出版年	ページ
伊藤雅之，青天目信，高橋悟，原宗嗣，白川哲夫，田村文誉，梶浦一郎，森崎市治郎		青天目信、伊藤雅之	レット症候群診療ガイドブック	大阪大学出版会	大阪	2015	
Meguro-Horike M, Horike S.	MMCT-Mediated Chromosome engineering technique applicable to functional analysis of lncRNA and nuclear dynamics.	S. Nakagawa, T. Hirose	Nuclear Bodies and Noncoding RNAs	Springer New York	New York	2015	277-289
松石豊次郎	PCD（一次性〈全身性〉カルニチン欠損症）	杉江秀夫	代謝性ミオパチー	診断と治療社	東京	2014	101-104
目黒牧子，堀家慎一	発達障害の遺伝学から明らかとなる多彩なエピジェネティクスの役割		エピジェネティクスの産業応用	シーエムシー出版		2014	
松石豊次郎	27. Rett 症候群. 稀少難治てんかん診療マニュアル	大槻泰介、須貝研司、小国弘量、井上有史、永井利三郎	疾患の特徴と診断のポイント	診断と治療社	東京	2013	84-87
伊藤雅之	てんかんの病理	辻　貞俊	最新医学別冊. 新しい診断と治療の ABC 74. てんかん	最新医学社	大阪	2012	72-82

雑誌

発表者氏名	論文タイトル名	発表誌名	巻号	ページ	出版年
Aono Y, Taguchi H, Saigusa T, Uchida T, Takada K, Takiguchi H, Shirakawa T, Shimizu N, Koshikawa N, Cools AR.	Simultaneous activation of the α1A-, α1B- and α1D-adrenoceptor subtypes in the nucleus accumbens reduces accumbal dopamine efflux in freely moving rats.	Behav Pharmacol	26	73-80	2015

Meguro-Horike M, Horike S.	MMCT-Mediated Chromosome engineering technique applicable to functional analysis of lncRNA and nuclear dynamics.	Methods Mol Biol	1262	277-289	2015
Nakamura H, Kato R, Shirakawa T, Koshikawa N, Kobayashi M	Spatiotemporal profiles of dental pulp nociception in rat cerebral cortex: An optical imaging study.	J Comp Neurol			2015 (in press)
奥田耕助, 田中輝幸	難治性てんかんを伴う神経発達障害の原因遺伝子CDKL5のシナプス伝達調節機構の解明に向けて	日本薬理学雑誌			2015 (in press)
Kumakura A, Takahashi S, Okajima K, Hata D	A haploinsufficiency of FOXG1 identified in a boy with congenital variant of Rett syndrome.	Brain Dev	36	725-729	2014
Hara M, Nishi Y, Yamashita Y, Hirata R, Takahashi S, Nagamitsu S, Hosoda H, Kangawa K, Kojima M, Matsuishi T	Relation between circulating levels of GH, IGF-1, ghrelin and somatic growth in Rett Syndrome.	Brain Dev	36	794-800	2014
高橋　悟	Rett症候群の病態理解 -病因遺伝子（MECP2, CDKL5, FOXG1）変異に関連した臨床的特徴について-	脳と発達	46	117-120	2014
Waga C, Asano H, Tsuchiya A, Itoh M, Goto Y, Kohsaka S, Uchino S.	Identification of novel SHANK3 transcript in the developing mouse neocortex.	J Neurochem	128	280-293	2014
Ohba C, Nabatame S, Iijima Y, Nishiyama K, Tsurusaki Y, Nakashima M, Miyake N, Tanaka F, Ozono K, Saitsu H, Matsumoto N.	De novo WDR45 mutation in a patient showing clinically Rett syndrome with childhood iron deposition in brain.	J Hum Genet	59(5)	292-5	2014
Yamasaki M, Okada R, Takasaki C, Toki S, Fukaya M, Natsume R, Sakimura K, Mishina M, Shirakawa T, Watanabe M.	Opposing role of NMDA receptor GluN2B and GluN2D in somatosensory development and maturation.	J Neurosci	34	11534-11548	2014
Sukigara S, Dai H, Nabatame S, Otsuki T, Hanai S, Honda R, Saito T, Nakagawa E, Kaido T, Sato N, Kaneko Y, Takahashi A, Sugai K, Saito Y, Sasaki M, Goto Y, Koizumi S, Itoh M.	Expression of Astrocyte-related Receptors in Cortical Dysplasia with Intractable Epilepsy.	J Neuropathol Exp Neurol	73	798-806	2014

Itoh M, Iwasaki Y, Ohno K, Inoue T, Hayashi M, Ito S, Matsuzaka T, Ide S, Arima M.	Nationwide survey of Arima syndrome: new diagnostic criteria from epidemiological analysis.	Brain Dev	36	388-393	2014
Matsuoka M, Nagamitsu S, Iwasaki M, Iemura A, Yamashita Y, Maeda M, Kitani S, Kakuma T, Uchimura N, Matsuishi T.	High incidence of sleep problems in children with developmental disorders: Results of a questionnaire survey in a Japanese elementary school.	Brain Dev	36	35-44	2014
Ohya T, Morita K, Yamashita Y, Egami C, Ishii Y, Nagamitsu S, Matsuishi T.	Impaired exploratory eye movements in children with Asperger's syndrome.	Brain Dev	36	241-247	2014
Shibuya I, Nagamitsu S, Okamura H, Ozono S, Chiba H, Ohya T, Yamashita Y, Matsuishi T.	High correlation between salivary cortisol awakening response and the psychometric profiles of healthy children.	Bio Psycol Social Med	8	9	2014
Tomonoh Y, Deshimaru M, Araki K, Miyazaki Y, Arasaki T, Tanaka Y, Kitamura H, Mori F, Wakabayashi K, Yamashita S, Saito R, Itoh M, Uchida T, Yamada J, Migita K, Ueno S, Kitaura H, Kakita A, Lossin C, Takano Y, Hirose S.	The Kick-In System: A Novel Rapid Knock-In Strategy.	PLoS ONE	9(2)	e88549	2013
Miyake K, Yang C, Minakuchi Y, Ohori K, Soutome M, Endoh K, Hirasawa T, Kazuki Y, Adachi N, Suzuki S, Itoh M, Goto Y, Andoh T, Kurosawa H, Oshimura M, Sasaki M, Toyoda A, Kubota T.	Comparison of genomic and epigenomic expression in monozygotic twins discordant for Rett syndrome.	PLoS ONE	8(6)	e66729	2013
Seki Y, Mizuochi T, Kimura A, Takahashi T, Ohtake A, Hayashi S, Morimura T, Ohno Y, Hoshina T, Ihara K, Takei H, Nittono H, Kurosawa T, Homma K, Hasegawa T, Matsuishi T.	Two neonatal cholestsis patients with mutations in the SRD5B1 (AKR1D1) gene: diagnosis and bile acid profiles during chenodeoxycholic acid treatment.	J Inherit Metab Dis	36	565-573	2013
伊藤雅之	レット症候群：自閉性障害をもつ特異な発達障害.	SRL宝函	34(2)	28-39	2013

松石豊次郎	レット症候群研究の現況と展望.	日本臨床	7 (11)	2043-53	2013
田中輝幸, 奥田耕助.	小児の難治性てんかんと CDKL5.	Clin Neurosci	31	699-702	2013
Sakakibara T, Saito T, Otsuk T, Takahashi A, Kaneko Y, Kaido T, Saito Y, Sato N, Nakagawa E, Sugai K, Sasaki M, Goto Y, Itoh M.	Delayed maturation of neurons of focal cortical dysplasia IIA and IIB: consideration from specific neocortical-layer marker expression.	J Neuropathol Exp Neurol	71	741-749	2012
Itoh M, Tahimic CGT, Ide S, Otsuki A, Sasaoka T, Noguchi S, Oshimura M, Goto Y, Kurimasa A.	Methyl CpG-binding protein isoform MeCP2_e2 is dispensable for phenotypes but essential for embryo viability and placenta development.	J Biol Chem	287	13859-13867	2012
Sakakibara T, Sukigara S, Otsuki T, Takahashi A, Kaneko Y, Kaido T, Yuko Saito Y, Sato N, Nakagawa E, Sugai K, Sasaki M, Goto Y, Itoh M.	Imbalance of interneuron distribution between neocortex and basal ganglia: Consideration of epileptogenesis of focal cortical dysplasia.	J Neurol Sci	323	128-133	2012
Mizuochi T, Kimura A, Tanaka A, Muto A, Nittono H, Seki Y, Takahashi T, Kurosawa T, Kage M, Takikawa H, Matsuishi T.	Characterization of urinary bile acids in a pediatric BRIC-1 patient: Effect of rifampicin treatment.	Clin Chim Acta	413	1301-1304	2012
Okabe Y, Takahashi T, Mitsumasu C, Kosai K, Tanaka E, Matsuishi T.	Alterations of Gene Expression and Glutamate Clearance in Astrocytes Derived from an MeCP2-null Mouse Model of Rett Syndrome.	PloS ONE	7(4)	e35354	2012
Takei H, Song L, Ebihara K, Shirakawa T, Koshikawa N, Kobayashi M.	Histaminergic effects on the frequency of repetitive spike firing in rat insular cortex.	Neurosci Lett	518	55-59	2012
Takahashi S, Matsumoto N, Okayama A, Suzuki N, Araki A, Okajima K, Tanaka H, Miyamoto A.	FOXG1 mutations in Japanese patients with the congenital variant of Rett syndrome.	Clin Genet	82	569-573	2012
Nagai M, Meguro-Horike M, Horike S.	Epigenetic defects related to assisted reproductive technologies: Large offspring syndrome (LOS).	DNA Methylation-from Genomics to Technology		167-182	2012

III. 研究成果の刊行物・別刷

THE JOURNAL OF BIOLOGICAL CHEMISTRY VOL. 287, NO. 17, pp. 13859–13867, April 20, 2012

Methyl CpG-binding Protein Isoform MeCP2_e2 Is Dispensable for Rett Syndrome Phenotypes but Essential for Embryo Viability and Placenta Development*[S]

Received for publication, October 2, 2011, and in revised form, February 26, 2012 Published, JBC Papers in Press, February 28, 2012, DOI 10.1074/jbc.M111.309864

Masayuki Itoh[‡1,2], **Candice G. T. Tahimic**[§1,3], **Shuhei Ide**[‡], **Akihiro Otsuki**[§], **Toshikuni Sasaoka**[¶], **Shigeru Noguchi**[‖4], **Mitsuo Oshimura**[§**], **Yu-ichi Goto**[‡], **and Akihiro Kurimasa**[§**]

From the [‡]*Department of Mental Retardation and Birth Defect Research, National Institute of Neuroscience, National Center of Neurology and Psychiatry, Kodaira 187–8502, Japan, the* [§]*Institute of Regenerative Medicine and Biofunction, Graduate School of Medical Science, and the* **21st Century Centers of Excellence Program, Research Core for Chromosome Engineering Technology, Tottori University, Yonago 683–8503, Japan, the* [¶]*Department of Laboratory Animal Science, Kitasato University School of Medicine, Sagamihara 252–0374, Japan, and the* [‖]*Signal Transduction Project, Kanagawa Academy of Science and Technology, Kawasaki 213–0012, Japan*

Background: There are two isoforms of *MeCP2*: *MeCP2_e1* and *_e2*. It is not known whether *MeCP2_e2* has specific functions *in vivo*.
Results: Deletion of *MeCP2_e2* results in no neurological phenotypes but confers a survival disadvantage to embryos and placenta defects.
Conclusion: *MeCP2_e2* functions in placenta development and embryo survival.
Significance: *MeCP2_e2* deletion results in a non-Rett syndrome phenotype but adversely affects embryo viability.

Methyl CpG-binding protein 2 gene (*MeCP2*) mutations are implicated in Rett syndrome (RTT), one of the common causes of female mental retardation. Two MeCP2 isoforms have been reported: *MeCP2_e2* (splicing of all four exons) and *MeCP2_e1* (alternative splicing of exons 1, 3, and 4). Their relative expression levels vary among tissues, with *MeCP2_e1* being more dominant in adult brain, whereas *MeCP2_e2* is expressed more abundantly in placenta, liver, and skeletal muscle. In this study, we performed specific disruption of the *MeCP2_e2*-defining exon 2 using the Cre-*loxP* system and examined the consequences of selective loss of MeCP2_e2 function *in vivo*. We performed behavior evaluation, gene expression analysis, using RT-PCR and real-time quantitative PCR, and histological analysis. We demonstrate that selective deletion of *MeCP2_e2* does not result in RTT-associated neurological phenotypes but confers a survival disadvantage to embryos carrying a *MeCP2_e2* null allele of maternal origin. In addition, we reveal a specific requirement for MeCP2_e2 function in extraembryonic tissue, where selective loss of MeCP2_e2 results in placenta defects and up-regulation of *peg-1*, as determined by the parental origin of the mutant allele. Taken together, our findings suggest a novel role for MeCP2 in normal placenta development and illustrate how paternal X chromosome inactivation in extraembryonic tissues confers a survival disadvantage for carriers of a mutant maternal *MeCP2_e2* allele. Moreover, our findings provide an explanation for the absence of reports on *MeCP2_e2*-specific exon 2 mutations in RTT. *MeCP2_e2* mutations in humans may result in a phenotype that evades a diagnosis of RTT.

Methyl CpG-binding protein 2 gene (*MeCP2*) mutations are implicated in Rett syndrome (RTT),[5] one of the common causes of female mental retardation (1, 2). RTT patients exhibit apparently normal early psychomotor development and then gradually lose previously acquired psychomotor skills. Stereotypic hand movements and microcephaly are also clinical features of this disorder (3). MeCP2 binds to methylated CpG dinucleotides and functions as a transcriptional repressor through its interactions with the Sin3A/histone deacetylase complex and the SWI/SNF chromatin remodeling complex (4–8). To date, two MeCP2 isoforms have been characterized. The first reported MeCP2 isoform, referred to as MeCP2_e2 (translational start site in exon 2; also known as MeCP2A or MeCP2β), is generated by splicing of all four exons and has a translation start site in the middle of exon 2. The more recently discovered isoform, MeCP2_e1 (translational start site in exon 1; also known as MeCP2B or MeCP2α), results from alternative splicing of exons 1, 3, and 4 and has a translation start site in exon 1 (9, 10). Their relative expression levels vary among tissues, with MeCP2_e1 being more dominant in adult brain, whereas MeCP2_e2 is expressed more abundantly in placenta,

* This work was supported by Ministries of Health, Labor, and Welfare Grants 15B-3, 18A-3, H21-Nanchi-Ippan-110, and H22-Nanchi-Ippan-133 and by Ministries of Education, Culture, Science, Sports, and Technology of Japan Grant 18390304.
[S] This article contains supplemental Fig. 1.
[1] Both authors contributed equally to this work.
[2] To whom correspondence should be addressed: 4-1-1 Ogawahigashi, Kodaira, Tokyo 187-8502, Japan. Tel.: 81-423461713; Fax: 81-423461743; E-mail: itoh@ncnp.go.jp.
[3] Recipient of a Japanese Government Research Scholarship. Present address: Endocrine Unit, San Francisco Veterans Affairs Medical Center, San Francisco, CA 94121.
[4] Present address: Pharmaceuticals Analysis Group, Food Analysis and Safety Assessment Center, Food Technology Research Laboratories, R&D Division, Meiji Co. Ltd., Odawara 250–0862, Japan.
[5] The abbreviations used are: RTT, Rett syndrome; TRE, tetracycline-responsive promoter; tTA, tetracycline transactivator; XCI, X chromosome inactivation; PGK, phosphoglycerate kinase.

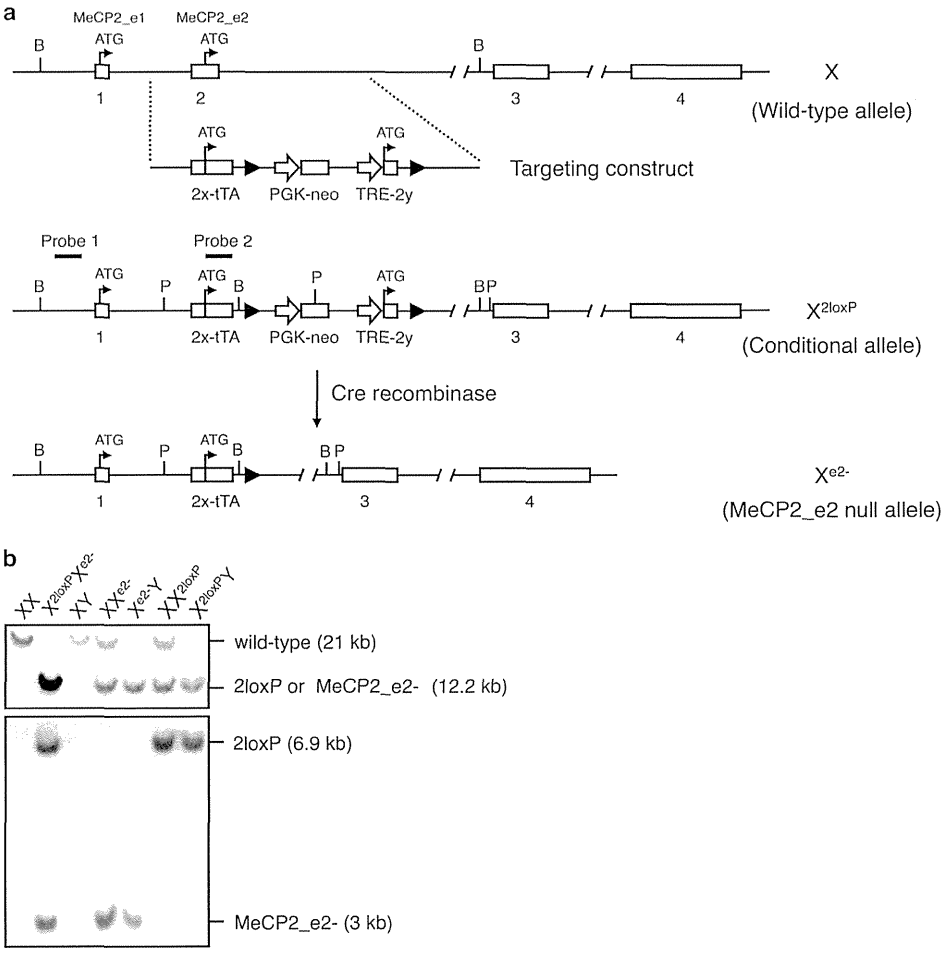

FIGURE 1. **Generation of *MeCP2_e2*-deficient mice.** *a*, strategy for selective targeting of *MeCP2_e2*. Transcription start sites for *MeCP2_e2* and *MeCP2_e1* before and after exon 2 disruption are shown. *loxP* sites are denoted as *filled triangles*. Relative location of probes for Southern hybridization, and positions of restriction enzymes BamHI (*B*) and PvuII (*P*) are indicated. Crossing of *MeCP2_e2* conditional mice with Nestin-Cre deleter mice results in the excision of the transcriptional start site of *MeCP2_e2* and the creation of the *MeCP2_e2* null allele, not only in neuronal cells but also in the germ line. Note that the transcriptional start of *MeCP2_e1* remains intact after disruption of the *MeCP2* locus. *b*, *MeCP2_e2* wild-type and mutant alleles as differentiated by two sets of Southern hybridization. For the first screening (*top*), genomic DNA was digested with BamHI and probed to visualize the presence of the targeted MeCP2 locus containing the exon 2x-tTA sequence. In the second screening (*bottom*), PvuI-digested genomic DNA was probed to differentiate between the conditional (X^{2loxP}) and null (X^{e2-}) alleles. Approximate band sizes are indicated in parentheses.

liver, and skeletal muscle (10). The most common MeCP2 mutations in RTT occur in exons shared by both isoforms (11). However, no mutation in the *MeCP2_e2*-defining exon 2 has ever been reported in RTT. In this study, we performed specific disruption of the *MeCP2_e2*-defining exon 2 using the Cre-*loxP* system and examined the consequences of selective loss of MeCP2_e2 function *in vivo*.

EXPERIMENTAL PROCEDURES

Selective Targeting of MeCP2_e2—The *MeCP2_e2* null allele was generated by Cre recombinase-mediated excision of exon 2 in *MeCP2_e2* conditional mice (Fig. 1). MeCP2 sequences were either directly derived or amplified from genomic DNA obtained from CJ7 ES cells or a BAC clone carrying the MeCP2 locus. The 5′-end of the targeting vector consisted of a 1.2-kb region possessing homology to intron 1 and was generated by high fidelity PCR. The early part of exon 2 containing the untranslated region (referred to as exon 2x) was fused to the tetracycline transactivator (tTA) gene, having a stop codon and poly(A) sequence. The latter half of exon 2 (referred to as exon 2y) beginning from the ATG start site of MeCP2_e2 was placed under the control of the tetracycline-responsive promoter, TRE. A pair of *loxP* sites flanked this TRE-exon 2y sequence. A PGK-driven neomycin selection marker was positioned between the first *loxP* site and the TRE-2y region. The 3′ arm of the targeting vector consisted of a 5.9-kb EcoRI fragment derived from intron 2.

Generation of MeCP2_e2 Null Mice—A correctly targeted ES cell clone, confirmed by Southern blot analysis, was injected into 3.5-day postconception (dpc) C57BL/6J blastocysts. Approximately 10 ES cells were injected per blastocyst, and 20 blastocysts were transferred to each pseudopregnant recipient. The resulting chimeric offspring were intercrossed mice to generate F1 progeny. For deletion of MeCP2_e2, we crossed MeCP2_e2$^{+/2loxP}$ females with deleter mice carrying a Cre recombinase transgene under the control of the Nestin promoter. However, leaky expression from Nestin promoter-driven Cre recombinase induced a deletion in the germ line, resulting in progeny that carried the *MeCP2_e2* null allele

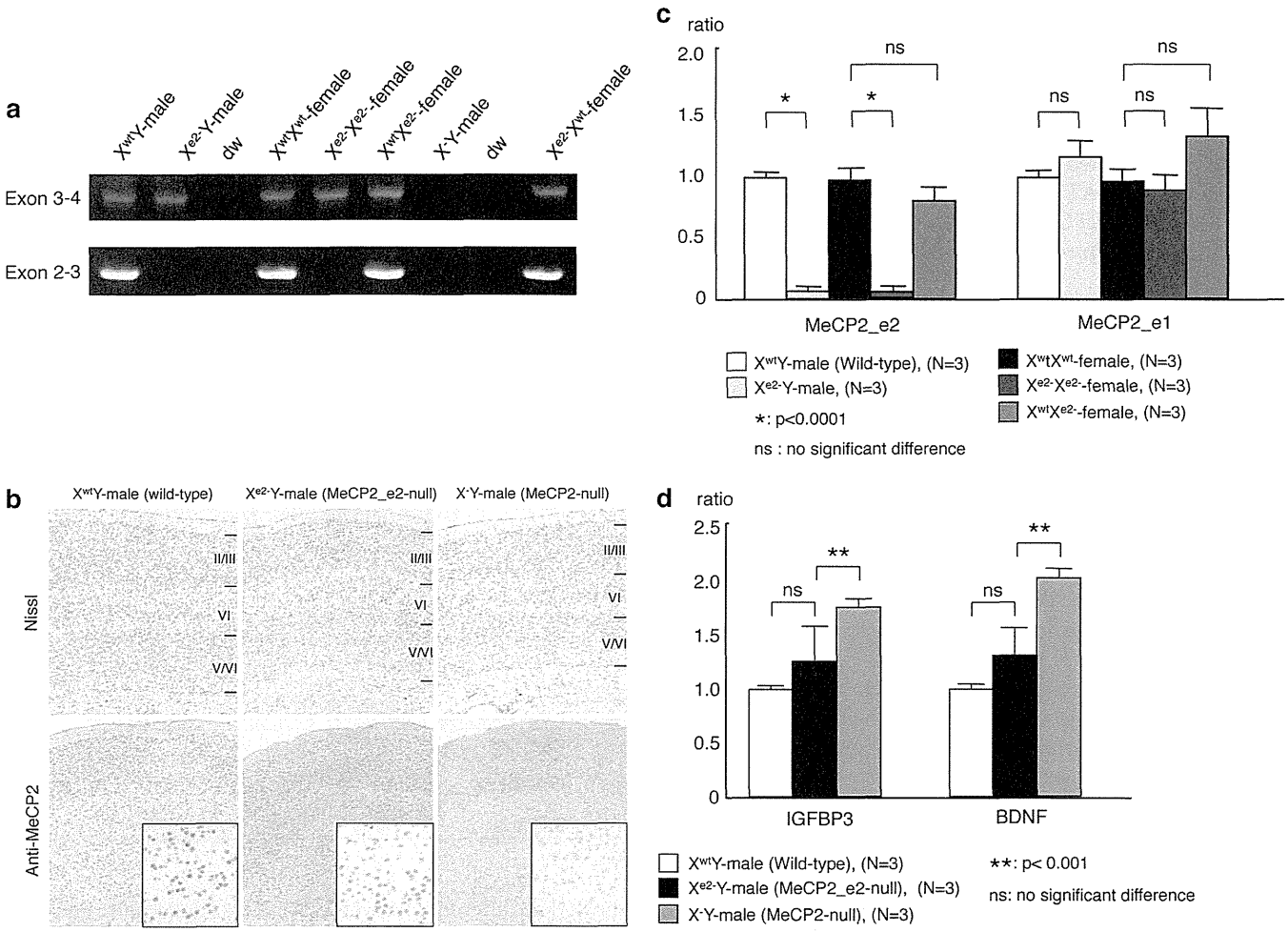

FIGURE 2. **Absence of RTT-associated phenotypes in *MeCP2_e2*-deficient mice.** *a*, reverse transcription PCR showing the selective loss of *MeCP2_e2* transcripts in brains of *MeCP2_e2* null males and females at P28. *b*, sections of P28 mouse brain were stained with cresyl violet to visualize neurons. Immunochemical staining was performed using anti-MeCP2 antibody. The *MeCP2*-deficient mouse, a previously reported *MeCP2_e2* and *MeCP2_e1* knockout (12), shows thinning of the cerebral cortex and no MeCP2-immunopositive cells. *MeCP2_e2* null mouse exhibits MeCP2-immunopositive cells in the cerebral cortex. *c*, real-time PCR analysis of *MeCP2_e2* and *MeCP2_e1* of P28 brains. The *MeCP2_e2*-deficient mouse shows *MeCP2_e1* expression but not *MeCP2_e2*, as indicated by the presence of exons 3 and 4 and the absence exons 2 and 3. *d*, quantitation of BDNF and IGFBP3 transcripts in P0 *MeCP2_e2*-deficient mice by real-time PCR. An $X^{wt}Y$ male mouse was used as a reference. Statistical analysis was performed using Student's *t* test at $p < 0.0001$ (*) and $p < 0.001$ (**). *Error bars*, S.D.

TABLE 1

Offspring distribution at 4 weeks of age; crossing of $X^{wt}X^{e2-}$ females and $X^{wt}Y$ males (maternal transmission of MeCP2_e2 null allele)

χ sum = 107.04, $p < 0.0001$. % Change = (% observed value − % expected value)/% expected value) × 100.

	$X^{wt}X^{wt}$	$X^{e2-}X^{wt}$	$X^{wt}Y$	$X^{e2-}Y$	Total
Observed	52 (27%)	27 (14%)	101 (53%)	12 (6%)	192
Estimated	48 (25%)	48 (25%)	48 (25%)	48 (25%)	192
% Change	8%	−44%	−112%	−76%	

TABLE 2

Offspring distribution at 4 weeks of age; crossing of $X^{wt}X^{e2-}$ females and $X^{e2-}Y$ males (biparental transmission of MeCP2_e2 null allele)

χ sum = 16.20, $p < 0.002$. % Change = (% observed value − % expected value)/% expected value) × 100.

	$X^{wt}X^{e2-}$	$X^{e2-}X^{e2-}$	$X^{wt}Y$	$X^{e2-}Y$	Total
Observed	11 (28%)	4 (10%)	20 (50%)	5 (12%)	40
Estimated	10 (25%)	10 (25%)	10 (25%)	10 (25%)	40
% Change	10%	−60%	100%	−50%	

(X^{e2-}). This population was expanded and used in succeeding experiments. Genotypes of the resulting progeny were assessed by an initial PCR screen followed by two sets of Southern blotting. The *MeCP2_e2* null allele was generated by Cre recombinase-mediated excision of exon 2 in *MeCP2_e2* conditional mice (Fig. 1). A previously reported MeCP2 null mouse, B6.129P2(C)-*Mecp2*$^{tm1.1Bird}$ (described as $MeCP2^{-/y}$), generated by targeted disruption of exons 3 and 4 (12), was obtained from Jackson Laboratory (Bar Harbor, ME) and used as a control for some of the experiments. All animal studies were performed with the approval of the Animal Care Committee of the National Institute of Neuroscience, National Center of Neurology and Psychiatry, Japan.

RT-PCR and Real-time Quantitative PCR—We prepared 3–8 fresh frozen brains and placentas of various genotypes at 13.5 dpc and postnatal days 0 (P0) and 28 (P28). Total RNA was isolated from mouse tissue using the RNeasy minikit (Qiagen, Valencia, CA) following the manufacturer's recommendations. We carried out reverse transcription with the First-Strand cDNA synthesis kit (Amersham Biosciences) or TaqMan

reverse transcription reagents (Applied Biosystems, Foster City, CA) using oligo(dT). Primer sequences and annealing conditions are as follows: for MECP2 exons 2 and 3, 5′-TTAGGGCTCAGGGAGGAAAA-3′ (forward) and 5′-CAAAATCATTAGGGTCCAAGG-3′ (reverse) with annealing temperature of 50 °C and expected PCR product size of 451 bp; for *MECP2* exons 3 and 4, 5′-ATTATCCGTGACCGGGGA-3′ (forward) and 5′-TGATGCTGCTGCCTTTGGT-3′ (reverse) with annealing temperature of 55 °C and an expected PCR product size of 354 bp.

For quantitative analysis, we carried out PCR amplifications using Universal PCR Master Mix (Applied Biosystems) according to the manufacturer's recommendations in a real-time ABI PRISM 7700 platform (Applied Biosystems). Relative transcript ratios were normalized to GAPDH RNA. Primers and probes for mouse *MeCP2* (common sequence of *MeCP2_e2* and *MeCP2_e1*), *MeCP2_e2*, *MAP2*, *IGFBP3*, and *BDNF* are available from Applied Biosystems. The probes 5′-CGCCGAGCGGAGGAG-3′ and 5′-CCTGGTCTTCTGACTTTTCTTCCA were designed to amplify a portion of the *MeCP2_e1* transcript, and a probe of CCTCCTCGCCTCCTCC-3′ was used. Sequence Detection System 1.7 software (Applied Biosystems) was used for analysis.

Immunohistochemical Analysis and TUNEL Assay—Tissues were fixed in 4% paraformaldehyde and then embedded in paraffin. Three-micrometer sections were prepared and stained with cresyl violet to visualize neurons. Purified MeCP2 antibody (provided by Dr. S. Kudo, Hokkaido Institute of Public Health, Sapporo, Japan), cleaved caspase-3 antibody (Chemicon International Inc., Temecula, CA), Peg-1 antibody (Atlas Antibodies AB, Stockholm, Sweden), and CRCX4 antibody (Abnova, Taipei, Taiwan) were used for immunohistological experiments. TUNEL assays were performed using terminal deoxynucleotidyltransferase (Roche Applied Science) following the manufacturer's recommendations.

Behavior Analysis—We performed tail suspension, footprinting, and open field analysis, using 4- or 5-week-old wild-type, MeCP2_e2^{-}, MeCP2_e2^{2loxP}, and MeCP2$^{-/y}$ males.

Statistical Analysis—Statistical analysis was performed using the χ^2 test. Animal crossings were performed to evaluate the effect of parent-specific transmission of the MeCP2_e2 null allele using appropriate sample sizes. Statistical significance of the expression levels was evaluated using Student's *t* test with a significance level of $p < 0.05$.

RESULTS AND DISCUSSION

MeCP2_e2-null Mouse Generation—We generated the *MeCP2_e2* mutant allele (X^{e2-}) by crossing mice carrying a tetracycline-inducible *MeCP2_e2* conditional allele (X^{2loxP}) with deleter mice carrying a Nestin-driven Cre recombinase transgene (Fig. 1). We observed germ line transmission of the *MeCP2_e2* null allele in some of the F3 generation (Fig. 1), probably resulting from leaky expression of Nestin-driven Cre recombinase in non-brain tissue. This subpopulation was expanded, and the F10 to F12 generations were used for the experiments in this study. We confirmed loss of MeCP2_e2 expression, whereas *MeCP2_e1* transcription remained intact in these animals (Fig. 2, *a* and *c*). Brain histological analysis showed no difference between *MeCP2_e2* null mouse and wild-type mice (Fig. 2*b*).

TABLE 3

Offspring distribution at 4 weeks of age; crossing of $X^{wt}X^{wt}$ females and $X^{e2-}Y$ males (paternal transmission of MeCP2_e2 null allele)

χ sum = 2.28, no significant difference. % Change = (% observed value − % expected value)/% expected value) × 100.

	$X^{wt}X^{e2-}$	$X^{wt}Y$	Total
Observed	50 (48%)	55 (52%)	105
Estimated	52.5 (50%)	52.5 (50%)	105
% Change	−4%	4%	

TABLE 4

Offspring distribution at 13.5 dpc; crossing of $X^{wt}X^{e2-}$ females and $X^{wt}Y$ males (maternal transmission of MeCP2_e2 null allele)

χ sum = 13.25, $p < 0.005$. % Change = (% observed value − % expected value)/% expected value) × 100.

	$X^{wt}X^{wt}$	$X^{e2-}X^{wt}$	$X^{wt}Y$	$X^{e2-}Y$	Total
Observed	36 (28%)	28 (22%)	46 (36%)	18 (14%)	128
Estimated	32 (25%)	32 (25%)	32 (25%)	32 (25%)	128
% Change	13%	−13%	44%	−44%	

TABLE 5

Offspring distribution at 13.5 dpc; crossing of $X^{wt}X^{wt}$ females and $X^{e2-}Y$ males (paternal transmission of MeCP2_e2 null allele)

χ sum = 2.28, no significant difference. % Change = (% observed value − % expected value)/% expected value) × 100.

	$X^{wt}X^{e2-}$	$X^{wt}Y$	Total
Observed	27 (61%)	17 (39%)	44
Estimated	22 (50%)	22 (50%)	44
% Change	23%	−23%	

Phenotypes and Expression Analyses of MeCP2_e2-null Mice—At birth, mice carrying *MeCP2_e2* mutant alleles were indistinguishable from wild-type littermates. They developed into fertile adults and did not display any neurological deficits observed in murine models for RTT (12, 13), indicating that MeCP2_e1 is sufficient to carry on the functions of MeCP2 in the brain. Moreover, mice carrying MeCP2_e2 mutant alleles lived as long as their wild-type siblings, over 2 years (data not shown). Immunohistochemical staining of brain tissue from $X^{e2-}Y$ and $X^{wt}X^{e2-}$ animals at 28 days of age revealed normal morphology of neuronal layers in contrast to the denser packaging of neurons in a previously reported RTT model wherein both MeCP2 isoforms have been knocked out (Fig. 2*b*) (14, 15). Taken together, these results demonstrate that loss of MeCP2_e1 function is not sufficient to cause RTT-associated neurological phenotypes.

To examine the implications of *MeCP2_e2* deficiency on MeCP2 transcriptional silencing activity, we checked mRNA levels of two MeCP2-regulated genes, insulin like growth factor binding protein 3 (*IGFBP3*) (16, 17) and brain-derived nerve growth factor (*BDNF*) (18). The mRNA levels of these genes in brains of $X^{e2-}Y$ mice did not significantly differ from those of age-matched wild-type males (Fig. 2*d*). In contrast, IGFBP3 and BDNF transcript levels increased by 1.6- and 2-fold, respectively, in the $X^{-}Y$ total MeCP2 knockout. These findings indi-

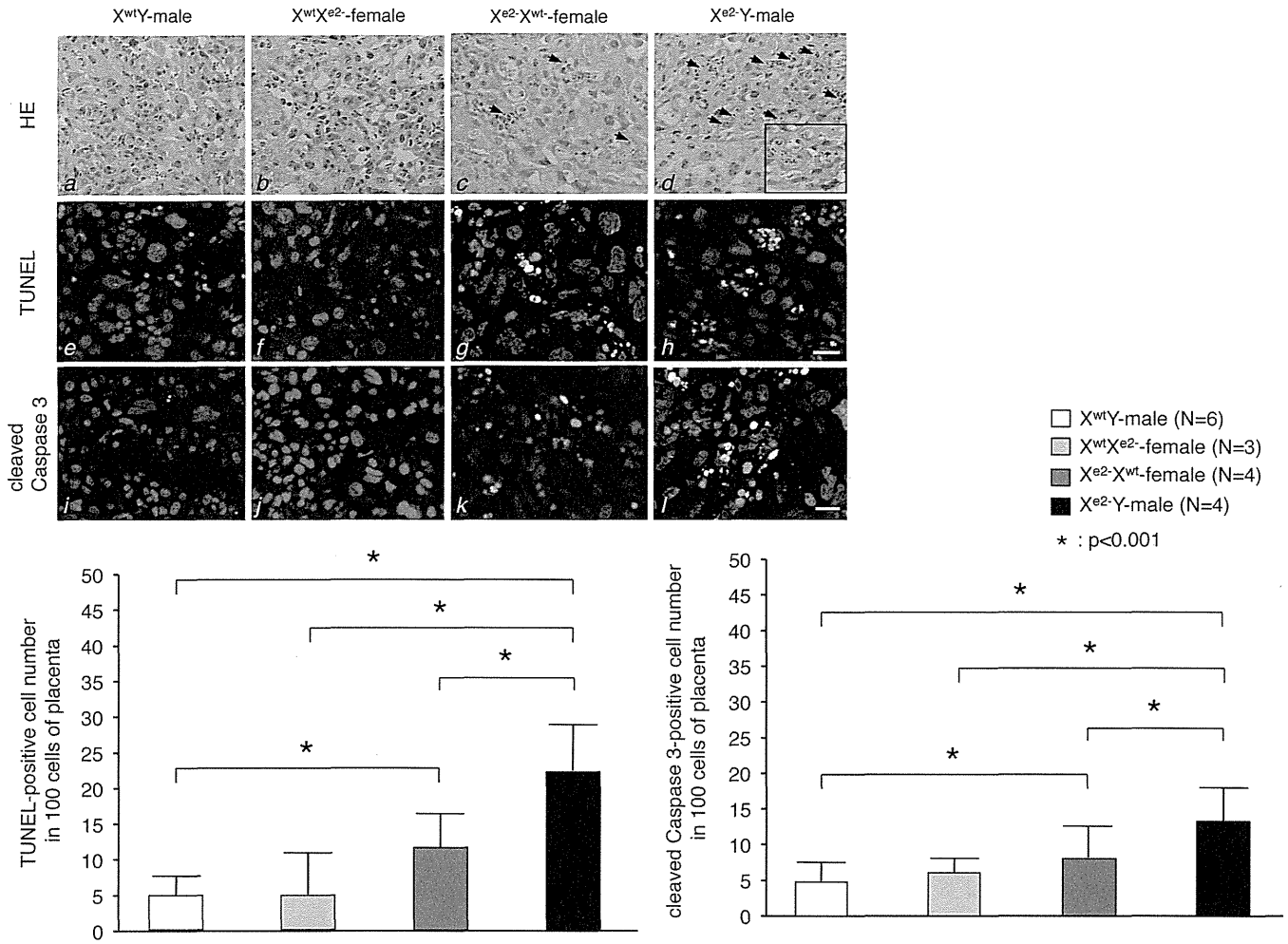

FIGURE 3. ***MeCP2_e2* deficiency results in placenta abnormalities.** The *top panels* (*a–d*) show placenta sections stained with hematoxylin and eosin. The *inset* shows the section at higher magnification. *Arrows* show apoptotic cells. The *middle panels* (*e–h*) show TUNEL staining of the same sections. Apoptotic nuclei appear as multiple spots (*yellow*), indicating DNA fragmentation. Propidium iodide was used as counterstain. The *bottom panels* (*i–l*) show cleaved caspase-3 immunostaining of the placenta. TUNEL-positive cells are indicated by *arrows*. *Scale bar*, 25 μm. An increase in the number of TUNEL-positive cells and cleaved caspase 3-positive cells was observed in the placentas of $X^{e2-}X^{wt}$ and $X^{e2-}Y$ embryos having a maternal *MeCP2_e2* null allele (refer to *bar graphs* in *lower panel* for quantitation) *, $p < 0.001$; *brackets* and *asterisks* indicate significant differences. *Error bars*, S.D.

cate that MeCP2_e2 is not essential for mediating transcriptional silencing of MeCP2 target genes in the brain.

Parent-specific Effects of MeCP2_e2 Null Allele Birth Rates—We next examined whether *MeCP2_e2* deficiency mediated any other non-neuronal phenotype. Interestingly, we observed reduced births of progeny that carried *MeCP2_e2* null allele of maternal origin. Specifically, we found a 76% reduction in $X^{e2-}Y$ males and a 44% reduction in $X^{e2-}X^{wt}$ females born to $X^{wt}X^{e2-}$ female and wild-type male pairings (Table 1). Similarly, in $X^{e2-}X^{wt}$ and $X^{e2-}Y$ pairings, $X^{e2-}Y$ and $X^{e2-}X^{e2-}$ births were reduced by 50 and 60%, respectively (Table 2). In contrast, birth rates of $X^{wt}X^{e2-}$ females (having a paternal X^{e2-}) did not deviate from the expected values (Tables 2 and 3). We exclude the possibility that these were nonspecific effects resulting from toxicity of the tTA in the targeting vector because no such decreases in births were observed in an unrelated transgenic mouse model carrying the same vector backbone.[6] Taken together, these results point to an association between reduced embryo viability and a maternally transmitted *MeCP2_e2* null allele.

To further delineate the time period at which selection against embryos carrying maternal *MeCP2_e2* null alleles occurred, we examined the genotype distribution at 13.5 dpc and observed similar trends (Tables 4 and 5). Moreover, we did not find any evidence of resorbed embryos at this time point (data not shown). We also performed morphological assessment of the uterus at preimplantation and postimplantation stages and found no abnormalities in preimplantation sites and the implantation process (data not shown). Nevertheless, these findings suggest that the reduced number of embryos carrying a mutant maternal *MeCP2_e2* allele is due neither to a failure in implantation nor to embryo lethality at postimplantation but to reduced viability of the embryo prior to implantation or early embryonic lethality after implantation.

Maternally Transmitted MeCP2_e2 Null Allele Results in Apoptosis and Altered peg-1 Expression in Placenta—During early development of the female mammal, one of the two X chromosomes becomes transcriptionally inactive to allow dos-

[6] A. Otsuki and A. Kurimasa, unpublished results.

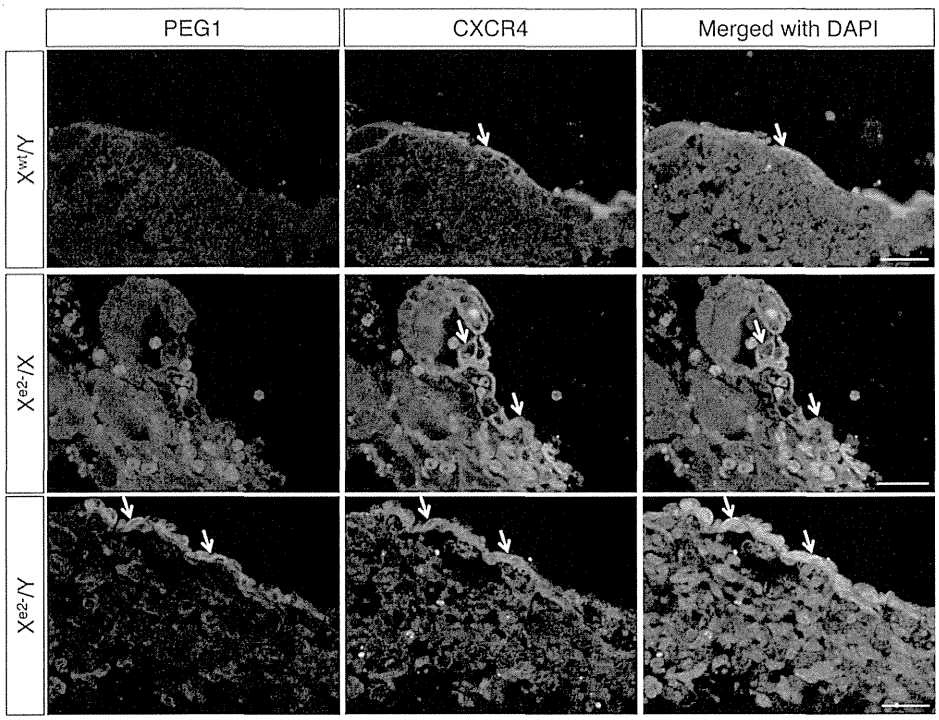

FIGURE 4. **Loss of maternal MeCP2_e2 results in failure to silence *peg-1* expression in trophoblast cells.** CXCR4 is a trophoblast cell marker. X^{wt}/Y and $X^{e2-}X^{wt}$ placenta have minimal *peg-1* expression, whereas X^{e2-}/Y placenta show elevated *peg-1* levels in trophoblast cells (*arrows*). *Scale bars*, 50 μm.

age compensation of X-linked genes (19, 20). In mouse extraembryonic lineages, such as placenta, the paternally derived X chromosome undergoes preferential inactivation, a phenomenon called imprinted paternal X chromosome inactivation (XCI) (21, 22). Hence, we examined the effect of *MeCP2_e2* deficiency in placenta tissue at 13.5 dpc. Interestingly, placentas of embryos carrying a maternal *MeCP2_e2* null allele exhibited increased apoptosis, which was more notable in placentas of males (Fig. 3). These TUNEL-positive cells expressed peg-1 (supplemental Fig. 1), an imprinted gene known to function in placenta development (23, 24). In contrast, very few apoptotic cells were observed in the placenta of $X^{wt}X^{e2-}$ embryos carrying a paternal *MeCP2_e2* null allele (Fig. 3). In addition, immunostaining revealed increased Peg-1 levels in cells expressing CXCR4, a trophoblast marker (25), in the placenta of animals carrying a maternal *MeCP2_e2* null allele (Fig. 4 and supplemental Fig. 1). Taken together, our results indicate that MeCP2_e2 is essential for the maintenance of *peg-1* silencing in trophoblast cells and that elevated expression of *peg-1* in the placenta has deleterious effects on cell survival.

We also examined transcript levels of *peg-1* and other imprinted genes involved in placenta function, such as *peg-3*, *igf-2*, and *h19* (23). Among these four genes, *peg-1* exhibited elevated transcript levels in the placenta of embryos carrying a maternal mutant allele (Fig. 5*a*), in concordance with our immunohistological findings. The mRNA levels of the other three genes were unchanged (Fig. 5*a*). In placentas of animals carrying the *MeCP2* two-isoform knock-out allele, *peg-1* expression was also elevated (Fig. 5*b*). The *peg-1* transcript levels were not due to deregulation of imprinting in placenta because imprinted paternal XCI was found to be intact in these animals (Fig. 5*c*). Rather, elevated *peg-1* transcript levels directly correlate with the loss of *MeCP2_e2* expression effected by imprinted paternal XCI. These findings indicate that *MeCP2_e2*-specific transcriptional silencing activity is essential for the regulation of *peg-1* expression and possibly of other genes in placenta.

The imprinted gene *peg-1*, located in murine chromosome 6, has been reported to play a role in angiogenesis in extraembryonic tissue (26). Mutations in *peg-1* have also been implicated in placenta failure (24, 25) and embryonic growth retardation (27). One group has reported that paternally expressed transcripts are associated with premature placenta (28). Interestingly, paternal transmission of a *peg-1* null allele in heterozygous mice results in diminished postnatal survival rates, whereas maternal transmission does not generate any remarkable phenotype (27, 29). It is clear from these reports that deregulation of *peg-1* expression or imprinting status has deleterious consequences on embryo viability and placenta function. Our current study demonstrates that MeCP2_e2 is an essential regulator of *peg-1* expression in extraembryonic tissue. As for how increased *peg-1* expression correlates with observed placenta defects in carriers of a maternal *MeCP2_e2* null allele, we propose a scenario wherein perturbations in *peg-1* expression results in disruption of biological pathways that involve Peg-1, leading to enhanced apoptosis in placenta. Peg-1 is a membrane-bound protein that is predicted to have lipase or acyltransferase activity based on sequence homology with the α/β-hydrolase superfamily of proteins (30). Lipid metabolism is a very important biological process and is critical for the developing embryo and placenta. We propose that loss of *MeCP2_e2* results in failure to transcriptionally silence *peg-1* in extraem-

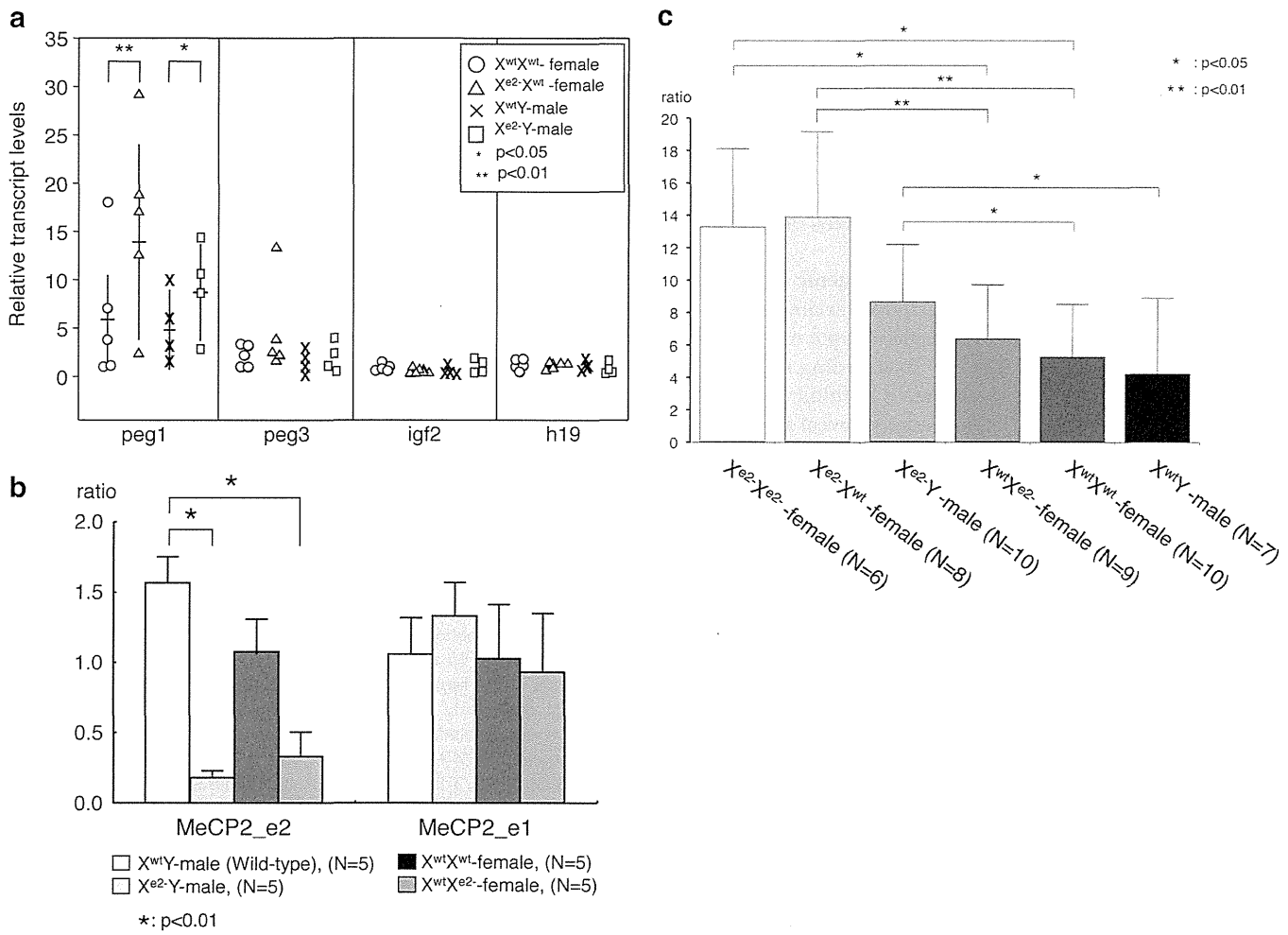

FIGURE 5. **Quantitative PCR analysis of placenta.** Shown are (*a*) placenta transcript levels of selected imprinted genes, *peg-1*, *peg-3*, *igf-2*, and *h19*, from 13.5 dpc embryos and (*b*) placenta transcript levels of peg-1 in *MeCP2_e2* and *MeCP2_e1* (two-isoform knockout) mutants. The *horizontal* and *vertical bars* of *peg-1* transcripts (*a*) show averages and S.D. of each genotype, respectively. *c*, *peg-1* expression in placentas of various genotypes. Maternally derived X^{e2-} allele up-regulated *peg-1* expression. *, $p < 0.05$; **, $p < 0.001$. *Brackets* and *asterisks* indicate significant differences. *Error bars*, S.D.

bryonic tissue, leading to increased Peg-1 enzymatic activity, aberrant regulation of Peg-1 binding partners or downstream targets, and, ultimately, apoptosis.

We have earlier stated that we found the implantation process to be normal for these animals. Moreover, at 13.5 dpc, there was no evidence of resorbed embryos, and the skewed embryo genotypes resembled that from postnatal analysis. These results, taken together with the increased number of apoptotic trophoblast cells and elevated *peg-1* expression in embryos carrying a maternal *MeCP2_e2* null allele, suggest that the loss of *MeCP2_e2* leads to trophoblast dysfunction during preimplantation through abnormal *peg-1* expression. Furthermore, we view the increase in apoptotic trophoblast cells as a persisting phenotype brought about by early perturbation of placenta gene expression. In mice, placental development begins in the blastocyst at embryonic day 3.5 when the trophectoderm layer becomes distinct from the inner cell mass (32). The trophoblast that lines the blastocyst plays an important role during attachment to the endometrium and in the formation of the placenta (31, 32). It has been reported by other groups that trophoblast dysfunction leads to disruption of placenta formation and reduction of birth number (31, 33). In our current study, we have shown that loss of *MeCP2_e2* results in a trophoblast defect that ultimately leads to reduced embryo viability.

Because some carriers of a mutant *MeCP2_e2* allele are born and develop into healthy adults, we hypothesize that the placenta abnormalities in these animals may have been overcome by *de novo MeCP2_e1* compensation or some other adaptation. In some types of extraembryonic cells, XCI can follow either a paternal or maternal pattern (34, 35). In somatic tissue, relaxation of imprinting occurs in certain pathological conditions (28, 36), and epigenetic heterogeneity at imprinted loci of autosomal chromosomes influences individual traits (37). The absence of *MeCP2_e2* correlated with up-regulation of *peg-1* expression, indicating a disturbance in regulation of downstream *MeCP2* gene targets. Although increased apoptosis in placenta could be used to explain the decreased viability of $X^{e2-}Y$ mice, this may also be interpreted as a way to eliminate functionally defective cells, thus contributing to the survival of some embryos.

The deleterious effects of *MeCP2* mutations have been viewed mostly in the context of somatic XCI patterns. A num-

ber of studies have addressed the contribution of XCI to the pathogenesis of *MeCP2* mutations (38, 39). It is suggested that XCI patterns may partly explain phenotypic variability in human RTT with *MeCP2* mutations (38) and in mouse RTT models (39). Our findings indicate that this is not the full picture and that paternal X chromosome inactivation in the extraembryonic lineage also contributes to the deleterious consequences of *MeCP2* mutations and, most likely, other X-linked gene mutations.

Recently, it has been reported that transgenic expression of either the *MeCP2_e1* or *MeCP2_e2* splice variant prevents the development of RTT-like neuronal phenotypic manifestations in a mouse model lacking *MeCP2*. This finding indicates that either *MeCP2* splice variant is sufficient to fulfill MeCP2 function in the mouse brain (40). Our findings reveal a novel mechanism for the pathogenesis of *MeCP2* mutations in extraembryonic tissue, wherein maternally inherited *MeCP2_e2* mutations result in placenta abnormalities that ultimately lead to a survival disadvantage for carriers of this mutant allele. Our study also provides an explanation for the absence of reports on *MeCP2_e2*-specific exon 2 mutations in RTT. It is conceivable that *MeCP2_e2* mutations in humans may result in a phenotype that evades a diagnosis of RTT. Moreover, the possible link between a novel genetic disorder characterized by reduced embryo viability and MeCP2 exon 2 mutations is a concept that merits further exploration. In summary, we have demonstrated that MeCP2_e2 is dispensable for RTT-associated neurological phenotypes. We have also discovered a novel requirement for MeCP2_e2 in placenta and embryo viability and have provided proof of existence of isoform-specific functions for two MeCP2 splicing variants.

Acknowledgments—We thank Dr. S. Kudo for the MeCP2 antibody and helpful suggestions and S. Kumagai and N. Tomimatsu for help with some of the experiments.

REFERENCES

1. Amir, R. E., Van den Veyver, I. B., Wan, M., Tran, C. Q., Francke, U., and Zoghbi, H. Y. (1999) Rett syndrome is caused by mutations in X-linked MECP2, encoding methyl-CpG-binding protein 2. *Nat. Genet.* **23,** 185–188
2. Rett, A. (1966) [On an unusual brain atrophy syndrome in hyperammonemia in childhood]. *Wien Med. Wochenschr.* **116,** 723–726
3. Hagberg, B., Aicardi, J., Dias, K., and Ramos, O. (1983) A progressive syndrome of autism, dementia, ataxia, and loss of purposeful hand use in girls. Rett's syndrome. Report of 35 cases. *Ann. Neurol.* **14,** 471–479
4. Lewis, J. D., Meehan, R. R., Henzel, W. J., Maurer-Fogy, I., Jeppesen, P., Klein, F., and Bird, A. (1992) Purification, sequence, and cellular localization of a novel chromosomal protein that binds to methylated DNA. *Cell* **69,** 905–914
5. Meehan, R. R., Lewis, J. D., and Bird, A. P. (1992) Characterization of MeCP2, a vertebrate DNA-binding protein with affinity for methylated DNA. *Nucleic Acids Res.* **20,** 5085–5092
6. Nan, X., Ng, H. H., Johnson, C. A., Laherty, C. D., Turner, B. M., Eisenman, R. N., and Bird, A. (1998) Transcriptional repression by the methyl-CpG-binding protein MeCP2 involves a histone deacetylase complex. *Nature* **393,** 386–389
7. Jones, P. L., Veenstra, G. J., Wade, P. A., Vermaak, D., Kass, S. U., Landsberger, N., Strouboulis, J., and Wolffe, A.P. (1998) Methylated DNA and MeCP2 recruit histone deacetylase to repress transcription. *Nat. Genet.* **2,** 187–191
8. Harikrishnan, K. N., Chow, M. Z., Baker, E. K., Pal, S., Bassal, S., Brasacchio, D., Wang, L., Craig, J. M., Jones, P. L., Sif, S., and El-Osta, A. (2005) Brahma links the SWI/SNF chromatin-remodeling complex with MeCP2-dependent transcriptional silencing. *Nat. Genet.* **37,** 254–264
9. Kriaucionis, S., and Bird, A. (2004) The major form of MeCP2 has a novel N terminus generated by alternative splicing. *Nucleic Acids Res.* **32,** 1818–1823
10. Mnatzakanian, G. N., Lohi, H., Munteanu, I., Alfred, S. E., Yamada, T., MacLeod, P. J., Jones, J. R., Scherer, S. W., Schanen, N. C., Friez, M. J., Vincent, J. B., and Minassian, B. A. (2004) A previously unidentified MECP2 open reading frame defines a new protein isoform relevant to Rett syndrome. *Nat. Genet.* **36,** 339–341
11. Bienvenu, T., and Chelly, J. (2006) Molecular genetics of Rett syndrome. When DNA methylation goes unrecognized. *Nat. Rev. Genet.* **7,** 415–426
12. Guy, J., Hendrich, B., Holmes, M., Martin, J. E., and Bird, A. (2001) A mouse Mecp2-null mutation causes neurological symptoms that mimic Rett syndrome. *Nat. Genet.* **27,** 322–326
13. Chen, R. Z., Akbarian, S., Tudor, M., and Jaenisch, R. (2001) Deficiency of methyl-CpG binding protein-2 in CNS neurons results in a Rett-like phenotype in mice. *Nat. Genet.* **27,** 327–331
14. Fukuda, T., Itoh, M., Ichikawa, T., Washiyama, K., and Goto, Y. (2005) Delayed maturation of neuronal architecture and synaptogenesis in cerebral cortex of Mecp2-deficient mice. *J. Neuropathol. Exp. Neurol.* **64,** 537–544
15. Dragich, J. M., Kim, Y. H., Arnold, A. P., and Schanen, N. C. (2007) Differential distribution of the MeCP2 splice variants in the postnatal mouse brain. *J. Comp. Neurol.* **501,** 526–542
16. Chang, Y. S., Wang, L., Suh, Y. A., Mao, L., Karpen, S. J., Khuri, F. R., Hong, W. K., and Lee, H. Y. (2004) Mechanisms underlying lack of insulin-like growth factor-binding protein-3 expression in non-small-cell lung cancer. *Oncogene* **23,** 6569–6580
17. Itoh, M., Ide, S., Takashima, S., Kudo, S., Nomura, Y., Segawa, M., Kubota, T., Mori, H., Tanaka, S., Horie, H., Tanabe, Y., and Goto, Y. (2007) Methyl CpG-binding protein 2 (a mutation of which causes Rett syndrome) directly regulates insulin-like growth factor binding protein 3 in mouse and human brains. *J. Neuropathol. Exp. Neurol.* **66,** 117–123
18. Chen, W. G., Chang, Q., Lin, Y., Meissner, A., West, A. E., Griffith, E. C., Jaenisch, R., and Greenberg, M. E. (2003) Derepression of BDNF transcription involves calcium-dependent phosphorylation of MeCP2. *Science* **302,** 885–889
19. Mak, W., Nesterova, T. B., de Napoles, M., Appanah, R., Yamanaka, S., Otte, A. P., and Brockdorff, N. (2004) Reactivation of the paternal X chromosome in early mouse embryos. *Science* **303,** 666–669
20. Sado, T., and Ferguson-Smith, A. C. (2005) Imprinted X inactivation and reprogramming in the preimplantation mouse embryo. *Hum. Mol. Genet.* **14,** R59–64
21. Takagi, N., and Sasaki, M. (1975) Preferential inactivation of the paternally derived X chromosome in the extraembryonic membranes of the mouse. *Nature* **256,** 640–642
22. Harper, M. I., Fosten, M., and Monk, M. (1982) Preferential paternal X inactivation in extraembryonic tissues of early mouse embryos. *J. Embryol. Exp. Morphol.* **67,** 127–135
23. Obata, Y., Kaneko-Ishino, T., Koide, T., Takai, Y., Ueda, T., Domeki, I., Shiroishi, T., Ishino, F., and Kono, T. (1998) Disruption of primary imprinting during oocyte growth leads to the modified expression of imprinted genes during embryogenesis. *Development* **125,** 1553–1560
24. Coan, P. M., Burton, G. J., and Ferguson-Smith, A. C. (2005) Imprinted genes in the placenta. A review. *Placenta* **26,** S10–S20
25. Wu, X., Li, D. J., Yuan, M. M., Zhu, Y., and Wang, M. Y. (2004) The expression of CXCR4/CXCL12 in first-trimester human trophoblast cells. *Biol. Reprod.* **70,** 1877–1885
26. Mayer, W., Hemberger, M., Frank, H. G., Grümmer, R., Winterhager, E., Kaufmann, P., and Fundele, R. (2000) Expression of the imprinted genes MEST/Mest in human and murine placenta suggests a role in angiogenesis. *Dev. Dyn.* **217,** 1–10
27. Lefebvre, L., Viville, S., Barton, S. C., Ishino, F., Keverne, E. B., and Surani, M. A. (1998) Abnormal maternal behavior and growth retardation associated with loss of the imprinted gene Mest. *Nat. Genet.* **20,** 163–169

28. Looijenga, L. H., Gillis, A. J., Verkerk, A. J., van Putten, W. L., and Oosterhuis, J. W. (1999) Heterogeneous X inactivation in trophoblastic cells of human full-term female placentas. *Am. J. Hum. Genet.* **64,** 1445–1452
29. Beechey, C. V. (2000) Peg1/Mest locates distal to the currently defined imprinting region on mouse proximal chromosome 6 and identifies a new imprinting region affecting growth. *Cytogenet. Cell Genet.* **90,** 309–314
30. Nikonova, L., Koza, R. A., Mendoza, T., Chao, P. M., Curley, J. P., Kozak, L. P. (2008) Mesoderm-specific transcript is associated with fat mass expansion in response to a positive energy balance. *FASEB J.* **22,** 3925–3937
31. Lee, K. Y., Jeong, J. W., Tsai, S. Y., Lydon, J. P., and DeMayo, F. J. (2007) Mouse models of implantation. *Trends Endcrinol. Metab.* **18,** 234–239
32. Watson, E. D., and Cross, J. C. (2005) Development of structures and transport functions in the mouse placenta. *Physiology* **20,** 180–193
33. Chaddha, V., Viero, S., Huppertz, B., and Kingdom, J. (2004) Developmental biology of the placenta and the origins of placental insufficiency. *Semin. Fetal Neonatal Med.* **9,** 357–369
34. Migeon, B. R., Wolf, S. F., Axelman, J., Kaslow, D. C., and Schmidt, M. (1985) Incomplete X chromosome dosage compensation in chorionic villi of human placenta. *Proc. Natl. Acad. Sci. U.S.A.* **82,** 3390–3394
35. Coutinho-Camillo, C. M., Brentani, M. M., Butugan, O., Torloni, H., and Nagai, M. A. (2003) Relaxation of imprinting of IGFII gene in juvenile nasopharyngeal angiofibromas. *Diagn. Mol. Pathol.* **12,** 57–62
36. Sakatani, T., Wei, M., Katoh, M., Okita, C., Wada, D., Mitsuya, K., Meguro, M., Ikeguchi, M., Ito, H., Tycko, B., and Oshimura, M. (2001) Epigenetic heterogeneity at imprinted loci in normal populations. *Biochem. Biophys. Res. Commun.* **283,** 1124–1130
37. Bourdon, V., Philippe, C., Martin, D., Verloès, A., Grandemenge, A., and Jonveaux, P. (2003) MECP2 mutations or polymorphisms in mentally retarded boys. Diagnostic implications. *Mol. Diagn.* **7,** 3–7
38. Shahbazian, M. D., Sun, Y., and Zoghbi, H. Y. (2002) Balanced X chromosome inactivation patterns in the Rett syndrome brain. *Am. J. Med. Genet.* **111,** 164–168
39. Young, J. I., and Zoghbi, H. Y. (2004) X-chromosome inactivation patterns are unbalanced and affect the phenotypic outcome in a mouse model of rett syndrome. *Am. J. Hum. Genet.* **74,** 511–520
40. Kerr, B., Soto, C. J., Saez, M., Abrams, A., Walz, K., and Young, J. I. (2012) Transgenic complementation of MeCP2 deficiency. Phenotypic rescue of Mecp2-null mice by isoform-specific transgenes. *Eur. J. Hum. Genet.* **20,** 69–76

Alterations of Gene Expression and Glutamate Clearance in Astrocytes Derived from an MeCP2-Null Mouse Model of Rett Syndrome

Yasunori Okabe[1,2], Tomoyuki Takahashi[1,3]*, Chiaki Mitsumasu[1,3], Ken-ichiro Kosai[1,3,4], Eiichiro Tanaka[1,2], Toyojiro Matsuishi[1,3]

1 Division of Gene Therapy and Regenerative Medicine, Cognitive and Molecular Research Institute of Brain Diseases, Kurume University, Kurume, Japan, **2** Department of Physiology, Kurume University of Medicine, Kurume, Japan, **3** Department of Pediatrics, Kurume University of Medicine, Kurume, Japan, **4** Department of Gene Therapy and Regenerative Medicine, Advanced Therapeutics Course, Kagoshima University Graduate School of Medical and Dental Sciences, Kagoshima, Japan

Abstract

Rett syndrome (RTT) is a neurodevelopmetal disorder associated with mutations in the methyl-CpG–binding protein 2 (MeCP2) gene. MeCP2-deficient mice recapitulate the neurological degeneration observed in RTT patients. Recent studies indicated a role of not only neurons but also glial cells in neuronal dysfunction in RTT. We cultured astrocytes from MeCP2-null mouse brain and examined astroglial gene expression, growth rate, cytotoxic effects, and glutamate (Glu) clearance. Semi-quantitative RT-PCR analysis revealed that expression of astroglial marker genes, including GFAP and S100β, was significantly higher in MeCP2-null astrocytes than in control astrocytes. Loss of MeCP2 did not affect astroglial cell morphology, growth, or cytotoxic effects, but did alter Glu clearance in astrocytes. When high extracellular Glu was added to the astrocyte cultures and incubated, a time-dependent decrease of extracellular Glu concentration occurred due to Glu clearance by astrocytes. Although the shapes of the profiles of Glu concentration versus time for each strain of astrocytes were grossly similar, Glu concentration in the medium of MeCP2-null astrocytes were lower than those of control astrocytes at 12 and 18 h. In addition, MeCP2 deficiency impaired downregulation of excitatory amino acid transporter 1 and 2 (EAAT1/2) transcripts, but not induction of glutamine synthetase (GS) transcripts, upon high Glu exposure. In contrast, GS protein was significantly higher in MeCP2-null astrocytes than in control astrocytes. These findings suggest that MeCP2 affects astroglial genes expression in cultured astrocytes, and that abnormal Glu clearance in MeCP2-deficient astrocytes may influence the onset and progression of RTT.

Citation: Okabe Y, Takahashi T, Mitsumasu C, Kosai K-i, Tanaka E, et al. (2012) Alterations of Gene Expression and Glutamate Clearance in Astrocytes Derived from an MeCP2-Null Mouse Model of Rett Syndrome. PLoS ONE 7(4): e35354. doi:10.1371/journal.pone.0035354

Editor: Nicoletta Landsberger, University of Insubria, Italy

Received October 26, 2011; **Accepted** March 14, 2012; **Published** April 20, 2012

Funding: This work was supported in part by a Grant-in-Aid for Scientific Research (C) and a Grant-in-Aid for Young Scientists (B) from the Japan Society for the Promotion of Science. The funders had no role in study design, data collection and analysis, decision to publish, or preparation of the manuscript.

Competing Interests: The authors have declared that no competing interests exist.

* E-mail: takahashi_tomoyuki@kurume-u.ac.jp

Introduction

Rett syndrome (RTT) is a neurodevelopmetal disorder that affects one in 15,000 female births, and represents a leading cause of mental retardation and autistic behavior in girls [1,2]. Mutations in the methyl-CpG–binding protein 2 (MeCP2) gene, located in Xq28, have been identified as the cause for the majority of clinical RTT cases [3]. Knockout mouse models with disrupted MeCP2 function mimic many key clinical features of RTT, including normal early postnatal life followed by developmental regression that results in motor impairment, irregular breathing, and early mortality [4,5,6]. MeCP2 dysfunction may thus disrupt the normal developmental or/and physiological program of gene expression, but it remains unclear how this might result in a predominantly neurological phenotype.

In several RTT mouse models, a conditional knockout that is specific to neural stem/progenitor cells or postmitotic neurons results in a phenotype that is similar to the ubiquitous knockout, suggesting that MeCP2 dysfunction in the brain and specifically in neurons underlies RTT [1,6,7]. Recent studies have demonstrated that mice born with RTT can be rescued by reactivation of neuronal MeCP2 expression, suggesting that the neuronal damage can be reversed [1,6]. In addition, several studies using in vitro cell culture systems also indicate that MeCP2 may play a role in processes of neuronal maturation including dendritic growth, synaptogenesis, and electrophysiological responses [1,7]. These data support the idea that MeCP2 deficiency in neurons is sufficient to cause an RTT-like phenotype. However, emerging evidence now indicates that MeCP2 deficiency in glia may also have a profound impact on brain function [8,9,10,11,12,13]. Brain magnetic resonance (MR) studies in MeCP2-deficient mice demonstrated that metabolism in both neurons and glia is affected [8]. Furthermore, in vitro co-culture studies have shown that MeCP2-deficient astroglia non-cell-autonomously affect neuronal dendritic growth [9,10]. In addition, MeCP2-deficient microglia cause dendritic and synaptic damage mediated by elevated glutamate (Glu) release [11]. Very recent studies have indicated that re-expression of MeCP2 in astrocytes of MeCP2-deficient mice significantly improves locomotion, anxiety levels, breathing patterns, and average lifespan, suggesting that astrocyte dysfunc-

tion may be involved in the neuropathology and characteristic phenotypic regression of RTT [13].

Astrocytes regulate the extracellular ion content of the central nervous systems (CNS); they also regulate neuron function, via production of cytokines, and synaptic function, by secreting neurotransmitters at synapses [14,15]. Moreover, a major function of astrocytes is efficient removal of Glu from the extracellular space, a process that is instrumental in maintaining normal interstitial levels of this neurotransmitter [16]. Glu is a major excitatory amino acid; excess Glu causes the degeneration of neurons and/or seizures observed in various CNS diseases [14,17]. RTT is also associated with abnormalities in Glu metabolism, but these findings are controversial due to the limitations of the experimental strategies used. Two studies have demonstrated that Glu is elevated in the cerebrospinal fluid (CSF) of RTT patients [18,19]. MR spectroscopy in RTT patients also revealed elevations of the Glu and Gln peak [20,21]. On the other hand, an animal MR study reported that the levels of Glu and Gln were decreased in a mouse model of RTT [8]. A more recent study indicated that MeCP2-null mice have reduced levels of Glu, but elevated levels of Gln, relative to their wild-type littermates [22]. Another study reported increased Gln levels and Gln/Glu ratios in Mecp2 mutant mice, but no decreases in Glu levels [23]. Although these in vivo studies have explored the hypothesis that the Glu metabolic systems might be altered in RTT, no solid conclusions have yet been reached [24,25].

In this study, we investigated the contribution of MeCP2 to the physiological function of astrocytes. Our studies demonstrate that MeCP2 is not essential for the growth and survival of astrocytes, but is involved in astrocytic Glu metabolism via the regulation of astroglial gene expression.

Results

Characterization of MeCP2-null astrocytes

It was recently reported that MeCP2 is normally present not only in neurons but also in glia, including astrocytes, oligodenrocytes, and microglia [9,10,11]. To determine the roles of MeCP2 in astrocytes, we cultured cerebral cortex astrocytes from both wild-type ($MeCP2^{+/y}$) and MeCP2-null ($MeCP2^{-/y}$) mouse brains (Fig. 1). MeCP2-null astrocytes exhibited a large, flattened, polygonal shape identical to that of the wild-type astrocytes, suggesting that normal patterns of cellular recognition and contact were present. Semi-quantitative RT-PCR using primer sets that specifically amplify two splice variants, Mecp2 e1 and e2, showed that control astrocytes expressed Mecp2 e1 and e2, whereas neither Mecp2 variant was detectable in MeCP2-null astrocytes (Fig. 1A). We further confirmed expression of MeCP2 by immunocytochemical staining of astrocytes. In control samples, almost all GFAP-positive cells exhibited clear nuclear MeCP2 immunoreactivity in astrocytes, but no immunoreactivity was observed in MeCP2-null astrocytes (Fig. 1B).

MeCP2 has been reported to be involved in regulation of astroglial gene expression [26,27]. Consistent with this, GFAP levels were significantly higher in MeCP2-null astrocytes (Fig. 1A). Similarly, the expression of S100β, another astrocyte maturation marker, was significantly upregulated by MeCP2 deficiency (fold change of control = 1.0, GFAP: 2.195±0.504, n = 4 each, $p<0.05$; S100β: 2.779±0.329, n = 4 each, $p<0.01$). These results show that MeCP2 deficiency upregulates astroglial gene expression in astrocytes.

To compare the growth of the wild-type and MeCP2-null astrocytes, we counted total cell number at each passage (Fig. 2A). As passage number increased, the cell growth rate decreased dramatically for both types of astrocytes, ultimately culminating in senescence. There was no significant difference in growth rate between the control and MeCP2-null astrocyte cultures. We then measured astrocyte proliferation via BrdU incorporation assay (Fig. 2B and Fig. S1). After 2 h of BrdU treatment, the proportions of BrdU-incorporating cells were similar in the control and MeCP2-null astrocytes (6.635±1.655% in control versus 6.774±2.272% in MeCP2-null astrocytes, n = 4 each, p = 0.962). These results suggest that the absence of MeCP2 did not affect the proliferation of astrocytes in our culture condition.

We also tested the cytotoxic effects of hydrogen peroxide (H_2O_2), ammonium chloride (NH_4Cl), and glutamate (Glu), on astrocytes in our culture (Fig. 2C–E). In cultures derived from both wild-type and MeCP2-null strains, cell viability decreased with increasing concentrations of H_2O_2 and NH_4Cl. In contrast, in our culture conditions, we observed virtually 100% viability of both the control and MeCP2-null astrocytes after 24 h incubation with 10 mM Glu. Glu-induced gliotoxic effects have been previously reported by Chen et al. (2000), and are probably due to distinct differences in culture conditions, specifically the presence of glucose [28]. These results showed that H_2O_2 and NH_4Cl had a similar effect in both strains of astrocytes. There was no significant difference in viability between the control and MeCP2-null astrocyte cultures, indicating that MeCP2 deficiency did not affect astrocyte viability upon treatment with H_2O_2 and NH_4Cl.

Effects of glutamate on glutamate transporters and glutamine synthetase transcripts in MeCP2-null astrocytes

High extracellular Glu interferes with the expression of the astrocyte transporter subtypes, excitatory amino acid transporter 1(EAAT1)/glutamate/aspartate transporter (GLAST) and EAAT2/glutamate transporter-1 (GLT-1) [16,29]. To explore the effects of Glu on the expression of Glu transporter genes in cultured astrocytes from wild-type and MeCP2-null mouse brains, we asked whether treatment with 1.0 mM Glu altered expression of EAAT1 and EAAT2 mRNA, using a semi-quantitative RT-PCR assay (Fig. 3). EAAT1 and EAAT2 mRNA were expressed in both wild-type and MeCP2-null astrocytes, and were slightly higher in controls than in MeCP2-null astrocytes. Both EAAT1 and EAAT2 mRNA levels were altered in the control astrocytes after treatment with 1.0 mM Glu. EAAT1 mRNA levels decreased significantly in the wild-type astrocytes, both 12 h and 24 h after treatment with Glu (Fig. 3A). In contrast, EAAT1 decreased significantly in the MeCP2-null astrocytes, at 12 h but not 24 h after treatment. As with EAAT1, EAAT2 mRNA levels also decreased significantly in the control astrocytes, both 12 h and 24 h after treatment (Fig. 3B). However, EAAT2 decreased significantly in MeCP2-null astrocytes, 24 h but not 12 h after treatment. In addition, the effects of Glu on EAAT1 and EAAT2 relative fold expression at 12 h were altered in the MeCP2-null astrocytes (Fig. 3D: EAAT1; 0.618±0.033 in control versus 0.758±0.049 in MeCP2-null astrocytes, n = 10 each, $p<0.05$; Fig. 3E: EAAT2; 0.794±0.055 in control versus 0.964±0.048 in MeCP2-null astrocytes, n = 8 each, $p<0.05$). These results suggest that the loss of MeCP2 leads to transcriptional dysregulation of these genes, either directly or indirectly.

One important enzyme that plays a role in the Glu metabolic pathway is glutamine synthetase (GS) [17,29]. GS is mainly located in astrocytes; cultured astrocytes response to Glu with increased GS expression [17,29]. Consistent with this, 1.0 mM Glu treatment stimulated GS mRNA expression in both the wild-type and MeCP2-null astrocytes about 1.2-fold after 12 h but not 24 h (Fig. 3C). In addition, MeCP2 deficiency did not modify the

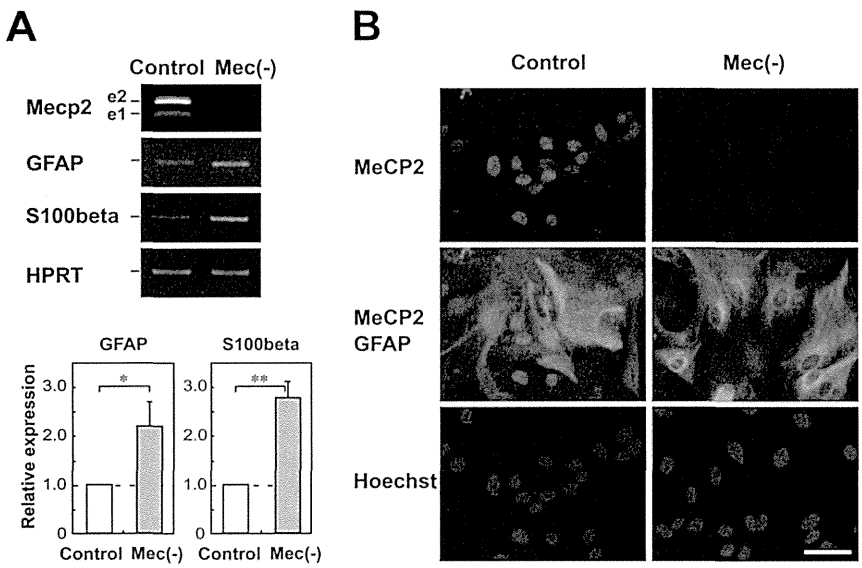

Figure 1. Characterization of assay cultures. A. Expression of astroglial genes in primary cultured cortical astrocytes. Semi-quantitative RT-PCR analysis of Mecp2 and astroglial genes was performed in wild-type (white column) and MeCP2-null (gray column) astrocytes. Mecp2 e1 and e2 were detectable in the wild-type astrocytes. The lower graphs show that the GFAP/HPRT or S100β/HPRT expression ratio in each genotype was normalized against the level in control astrocytes. Bars represent the means ± standard errors (SE) of samples from three independent experiments (*$p<0.05$). The expression of astroglial markers was significantly upregulated by MeCP2 deficiency. **B.** Expression of MeCP2 in the primary cultured cortical astrocytes. The astrocytes were immunostained with MeCP2 (green) and GFAP (red) as glial-specific astrocytic markers. Scale bars indicate 50 μm.
doi:10.1371/journal.pone.0035354.g001

effects of Glu on GS mRNA relative fold expression in cultured astrocytes (Fig. 3F, 1.245±0.054 in control versus 1.265±0.093 in MeCP2-null astrocytes, n = 6 each, p = 0.859). These results suggested that MeCP2 did not modify the expression of GS in the cultured astrocytes. Overall, the expression levels of GS mRNA did not differ between both strains of astrocytes following treatment with Glu.

Comparison of glutamate clearance between wild-type and MeCP2-null astrocytes

Because MeCP2 contributed to the transcriptional regulation of Glu metabolism-related genes in our culture systems, we next compared the Glu clearance capability of the wild-type and MeCP2-null astrocytes (Fig. 4A). The cell culture supernatants in both astrocyte cultures were collected at 3–24 h post incubation in culture media containing 1.0 mM Glu. After incubation in culture medium containing Glu, we identified a time-dependent reduction in Glu over 24 h of incubation in both strains of astrocytes. Although the shapes of the profiles of Glu concentration versus time for each strain of astrocytes were grossly similar, Glu concentration in the medium of MeCP2-null astrocytes were lower than those of control astrocytes at 12 and 18 h (12 h: control, 0.513±0.052 mM versus MeCP2-null, 0.395±0.022 mM, $p<0.05$; 18 h: control, 0.368±0.029 mM versus MeCP2-null, 0.125±0.007 mM, $p<0.01$, n = 6 each, Fig. 4A). The differences in Glu clearance were not due to changes in cell death of control astrocytes upon application of Glu (Fig. 2E). This indicates that Glu clearance by MeCP2-null astrocytes was more efficient than by control astrocytes.

The Glu transporters EAAT1 and EAAT2 are located primarily on astrocytes and are critical in maintaining extracellular Glu at safe levels [16]. Threo-beta-benzyloxyaspartate (TBOA) is a broad-spectrum glutamate transporter antagonist, affecting EAAT1 and EAAT2 [30]. UCPH-101 (2-amino-4-(4-methoxyphenyl)-7-(naphthalen-1-yl)-5-oxo-5,6,7,8-tetrahydro-4H-chromene-3-carbonitrile) and dihydrokainate (DHKA) are selective inhibitors for EAAT1 and EAAT2, respectively [30,31]. To investigate the functional Glu transporters in our astrocyte cultures, we analyzed three Glu transporter blockers (TBOA, UCPH-101, or DHKA) for their ability to alter the effects of Glu clearance (Fig. 4B–D). Glu clearance by the wild-type astrocytes was partially blocked by addition of TBOA and UCPH-101, but not DHKA. This suggests that EAAT1, but not EAAT2, plays a major role in Glu clearance under our astroglial culture conditions.

Effects of glutamate on glutamine synthetase and EAAT1 protein in MeCP2-null astrocytes

The initial set of experiments aimed to determine whether Glu modulate the translation of GS and EAAT1 protein (Fig. 5 and Fig. S2). GS protein was expressed in both wild-type and MeCP2-null astrocytes, and was significantly more abundant in MeCP2-null astrocytes (Fig. 5B: fold change of control = 1.0, 2.631±0.368, $p<0.01$). After 12 h exposure to 0.01–1.0 mM Glu, wild-type astrocytes exhibited a dose-dependent increase in GS protein levels (about 6-fold in 1.0 mM Glu treatment). Similar to its effect on the wild-type astrocytes, in the MeCP2-null astrocytes Glu exposure dose-dependently increased GS protein levels relative to untreated astrocytes (Fig. S2). We then examined the effect of 1.0 mM Glu on levels of GS protein, over a time course (Fig. 5A). GS expression was highest after 12 h exposure to 1.0 mM Glu, decreasing slightly by 24 h in both wild-type and MeCP2-null astrocytes. Densitometric analysis of the bands in three independent experiments demonstrated that GS protein in MeCP2-null astrocyte cultures was higher than in wild-type astrocytes, 12 h but not 24 h after treatment (Fig. 5B: fold change of control = 1.0, at 12 h: 1.421±0.139, $p<0.05$; at 24 h: 1.131±0.130, p = 0.354, n = 4 each). These results indicated that MeCP2 deficiency caused higher expression of GS protein in cultured astrocytes.

We also asked whether treatment with 1.0 mM Glu altered expression of EAAT1 protein. EAAT1 protein was expressed in

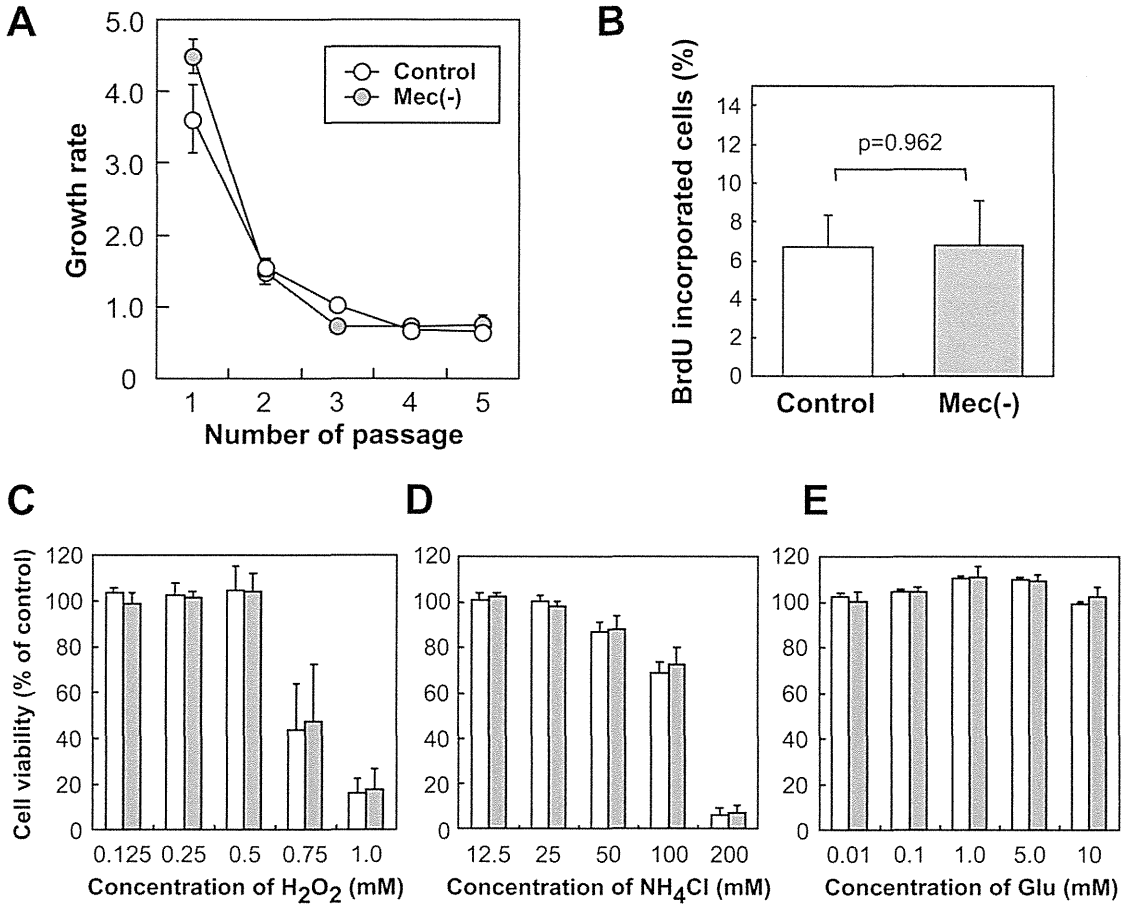

Figure 2. Cell growth and viability. A. Comparison of cell growth in wild-type and MeCP2-deficient astrocytes. As passage number increased, cell growth rate decreased dramatically in both strains of astrocytes. There was no significant difference in growth rate between the control and MeCP2-null astrocyte cultures. **B.** Quantification of BrdU-incorporating cells in control and MeCP2-null astrocytes. Astrocytes were cultured for 24 h and incubated with BrdU for 2 h. The graph shows the percentage of BrdU-incorporating cells in the control (white column) and MeCP2-deficient (gray column) astrocytes 2 h after BrdU exposure. The number of BrdU-incorporating cells is expressed as a percentage of the total number of Hoechst-stained cells (Fig. S1). Bars represent the means ± SE of the samples from four independent experiments. The ratio of BrdU-incorporating cells is similar in astrocytes taken from both control and MeCP2-null strains. **C–E.** Comparison of effects of various neurotoxins (**C,** H_2O_2; **D,** NH_4Cl; **E,** Glutamate) on control and MeCP2-null astrocytes. The graph shows the percentage of viability in the control (white column) and MeCP2-deficient (gray column) astrocytes after neurotoxin treatment at the indicated concentrations. Bars represent the means ± SE of samples from three independent experiments. The glial cultures showed no difference in viability between the control and MeCP2-null strains.
doi:10.1371/journal.pone.0035354.g002

both wild-type and MeCP2-null astrocytes, at levels that were similar in controls and MeCP2-null astrocytes. EAAT1 protein levels were altered in the wild-type astrocytes after treatment with 1.0 mM Glu. EAAT1 protein levels decreased significantly in the wild-type astrocytes, 24 h but not 12 h after treatment (Fig. 5C). In contrast, EAAT1 did not decrease in the MeCP2-null astrocytes, either 12 h or 24 h after treatment. In addition, the relative expression levels of EAAT1 24 h after treatment were lower in the wild-type than in the MeCP2-null culture, although the difference was not statistically significant (Fig. 5D: 12 h; 1.102±0.169 in control versus 1.096±0.142 in MeCP2-null astrocytes, n = 6 each, p = 0.979, 24 h; 0.456±0.123 in control versus 0.901±0.172 in MeCP2-null astrocytes, n = 5 each, p = 0.068). These results suggest that MeCP2 deficiency affects the expression of GS and EAAT1 protein, and that accelerated Glu clearance may result from dysregulation of GS and EAAT1 protein in MeCP2-null astrocytes.

Discussion

Recent studies suggest that glia, as well as neurons, cause neuronal dysfunction in RTT via non-cell-autonomous effects. Here, we have demonstrated that MeCP2 regulates the expression of astroglial marker transcripts, including GFAP and S100β in cultured astrocytes. In addition, MeCP2 is not essential for the cell morphology, growth, or viability; rather, it is involved in Glu clearance through the regulation of Glu transporters and GS in astrocytes. Altered astroglial gene expression and abnormal Glu clearance by MeCP2-null astrocytes may underlie the pathogenesis of RTT.

In this study, MeCP2-null astrocytes exhibited significantly higher transcripts corresponding to astroglial markers, including GFAP and S100β. Consistent with this, transcription of several astrocytic genes, including GFAP, is upregulated in RTT patients [26,32]. Indeed, MeCP2 binds to a highly methylated region in the GFAP and S100β in neuroepithlial cells [27,33]; ectopic

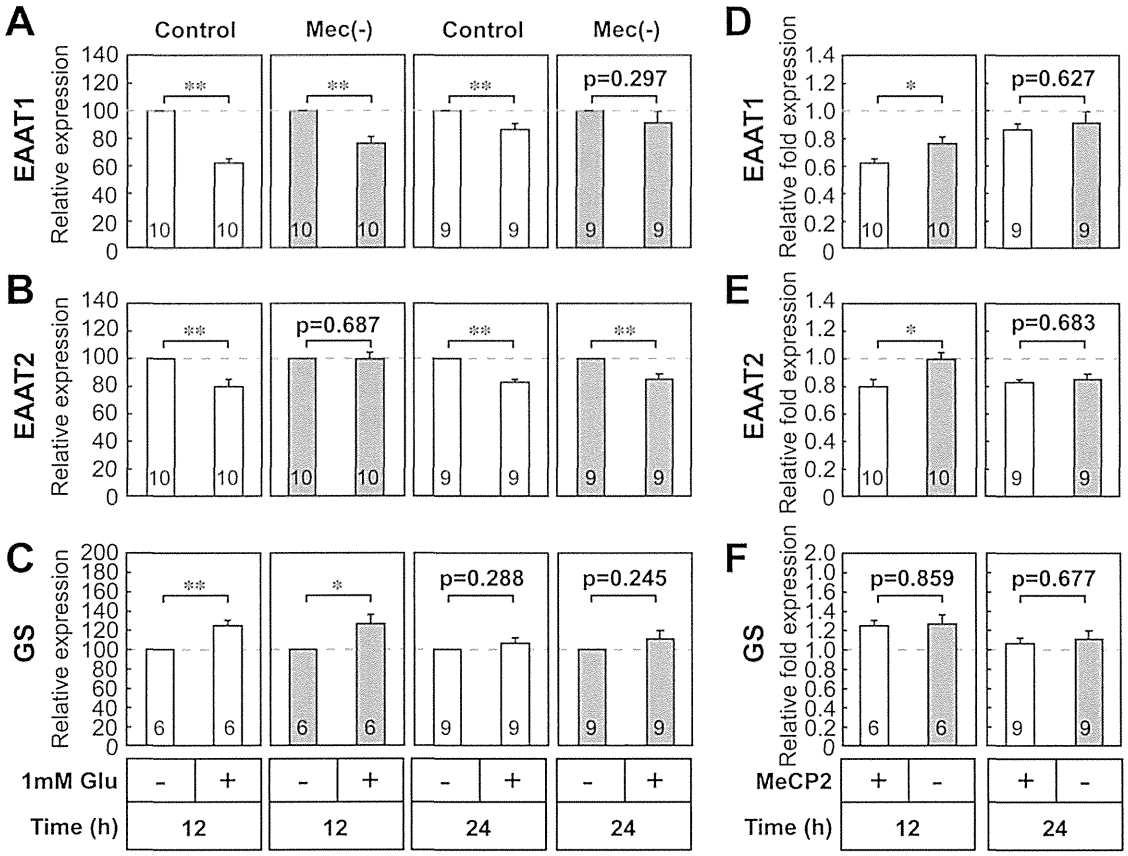

Figure 3. Effect of glutamate on glutamine synthetase and glutamate transporter gene expression in MeCP2-null astrocytes. A–C. Effects of Glu on Glu clearance-related genes in wild-type (white column) and MeCP2-null (gray column) astrocytes. Semi-quantitative RT-PCR analysis of Glu clearance-related genes, EAAT1 (**A**), EAAT2 (**B**), and GS (**C**), was performed in the control and MeCP2-null astrocytes 12 or 24 h after treatment with 1.0 mM Glu. The bands corresponding to PCR products were quantified by densitometry, normalized against HPRT levels, and expressed as % of controls (equals 100%). Bars represent the means ± SE of samples from 3–4 independent experiments (*$p<0.05$, **$p<0.01$). **D–F.** Comparison of the effects of Glu on EAAT1, EAAT2 or GS expression in the control and MeCP2-null astrocytes. The ratio of EAAT1/HPRT (**D**), EAAT2/HPRT (**E**) or GS/HPRT (**F**) in each treatment group was normalized against that of the non-treated astrocytes from each group. Bars represent the means ± SE of samples from 3–5 independent experiments (*$p<0.05$). Numbers in each column indicate the total number of samples analyzed.
doi:10.1371/journal.pone.0035354.g003

overexpression of MeCP2 inhibited the differentiation of neuroepithelial cells into GFAP-positive glial cells [34]. Our recent study in RTT-model ES cells also demonstrated that MeCP2 is involved in gliogenesis during neural differentiation via inhibition of GFAP expression [12]. Therefore, MeCP2 may be involved not only in the suppression of astroglial genes in neuroepithelial cells/neurons during neurogenesis, but also in the physiological regulation of astroglial gene expression in astrocytes.

We also demonstrated that MeCP2 is not essential for cell growth or cell viability in in vitro models of astrocyte injury, such as H_2O_2 oxidative stress and ammonia neurotoxicity. On the other hand, it has been reported that MeCP2 is involved in regulating astrocyte proliferation, and are probably due to distinct differences in culture conditions, specifically the presence of serum [10]. Consistent with these results, obvious neuronal and glial degeneration had not been observed in RTT [6,35]. These observations suggest that RTT is not caused by reduced cell numbers, but rather by dysfunction of specific cell types in the brain.

The regulation of Glu levels in the brain is an important component of plasticity at glutamatergic synapses, and of neuronal damage via excessive activation of Glu receptors [15,16]. Astrocytic uptake of Glu, followed by conversion of Glu to Glutamine (Gln), is the predominant mechanism of inactivation of Glu once it has been released in the synaptic cleft. This uptake involves two transporters, EAAT1/GLAST and EAAT2/GLT-1 [16]. Increases in extracellular Glu, present in many brain injuries, are sufficient to modulate the expression of Glu transporters and GS [16,29]. Furthermore, application of 0.5–1.0 mM Glu to cultured cortical astrocytes causes a decline in EAAT1/GLAST and EAAT2/GLT-1 expression [29]. Our present studies reveal that 1.0 mM extracellular Glu is sufficient to inhibit astroglial Glu transporter expression and to stimulate GS expression in control astrocytes. However, such regulatory influences on Glu transporters are impaired by MeCP2 deficiency. Therefore, MeCP2 may regulate the expression of Glu transporters under physiological conditions. Currently, little is known about the promoter regions of the main Glu transporters [36,37]. Promoter analysis in each gene may help to elucidate the complex regulations of astroglial genes by MeCP2.

On the other hand, in our culture conditions, MeCP2 deficiency did not impair the expression of GS transcripts in cultured astrocytes, but did affect the expression of GS protein. A very recent study has shown that defects in the AKT/mTOR pathway